Dynamics of pedogenic carbonate in the cropland of the North China Plain: Influences of intensive cropping and salinization

Tongping Lu[a], Xiujun Wang[a]*, Minggang Xu[b], Zhitong Yu[a,c], Yongming Luo[d], Pete Smith[e]

a. College of Global Change and Earth System Science, Beijing Normal University, Beijing, 100875, PR China

b. Institute of Agricultural Resources and Regional Planning, Chinese Academy of Agricultural Sciences, Beijing, 100081, PR China.

c. Qian Xuesen Laboratory of Space Technology, China Academy of Space Technology, Beijing, 100094, PR China

d. Institute of Soil Science, Chinese Academy of Sciences, Nanjing 210008, PR China

e. Institute of Biological and Environmental Sciences, University of Aberdeen, Aberdeen AB24 3UU, UK

*To whom correspondence should be addressed: Xiujun Wang (Ph: +86 10 58808201; Email: xwang@bnu.edu.cn)

Highlights

- PIC stock was significantly larger than SOC stock over 0-100 cm in the cropland of the North China Plain.
- There was a significant positive correlation between PIC and SOC stocks.
- Intensive cropping resulted in an increase in both SOC and PIC stocks in the semi-humid region.

Abstract

There is evidence of higher levels of pedogenic carbonate (PIC) than soil organic carbon (SOC) in cropland, and a positive relationship between PIC and SOC in salt-affected soils of arid and semi-arid regions. This study is designed to test the hypothesis that PIC is influenced by intensive cropping and salinization in semi-humid regions, in which soil carbonate (SIC) often exceeds SOC. We select a typical cropland with a maize-wheat rotation in the North China Plain, which covers two distinct regions, i.e. the Hebei Plain (HBP) under intensive cropping and the Yellow River Delta (YRD) under soil salinization. Our data show large variations in soil carbon stocks, with slightly higher values for PIC (3.9-14.5 kg C m^{-2}) relative to those of SOC (2.2-9.2 kg C m^{-2}) in the top 1 m. On average, SOC stock is 5.65 kg C m^{-2} in the YRD, which is slightly lower than in the HBP (6.21 kg C m^{-2}); SIC is significantly higher in the YRD (16.9 kg C m^{-2}) relative to the HBP (13.7 kg C m^{-2}). However, PIC stock is smaller in the YRD (8.67 kg C m^{-2}) relative to the HBP (9.41 kg C m^{-2}). Despite no clear SIC-SOC relationship, there exists a significant positive correlation ($P < 0.01$) between PIC and SOC stocks in the study area. The PIC:SOC ratio is generally greater than one over a 0-100 cm layer in the majority of croplands in the north China, with larger ratios in the salt-affected soils. Our analyses suggest that the formation and storage of PIC are regulated by levels of SOC and Ca^{2+}/Mg^{2+} in soil profiles, and there is large potential for enhancing carbon sequestration as carbonate under intensive cropping through sound management in the cropland of arid, semi-arid and semi-humid regions.

.

Keywords Pedogenic carbonate; Soil organic carbon; Cropland; Salts; North China Plain; Carbon isotope

1. Introduction

Soil carbon is the largest carbon pool in the terrestrial ecosystem, which exceeds the sum of carbon storage in the biosphere and atmosphere. Soil carbon mainly includes organic carbon (SOC) and inorganic carbon (SIC). There have been many studies on SOC dynamics because of its role in the agricultural management and the global carbon cycle. However, SIC has received much less attention despite its wide distribution in arid and semi-arid lands.

Land use type has a large influence on soil carbon dynamics (Wu *et al.*, 2003; Mikhailova and Post, 2006; Wu *et al.*, 2009; Andriamananjara *et al.*, 2016). While studies have shown higher SOC levels in forest and grasslands than in croplands (Don *et al.*, 2010; Saha *et al.*, 2011; Phillips *et al.*, 2015), there is evidence of significantly higher levels of both SOC and SIC in cropland than in native lands in the northwest China (Wang *et al.*, 2015a). On the other hand, a significant positive correlation between SIC and SOC has been reported for various ecosystems in north China, including cropland (Wang *et al.*, 2015b; Guo *et al.*, 2016; Shi *et al.*, 2017), shrub land (Su *et al.*, 2010; Zhang *et al.*, 2010), and afforestation soil (Gao *et al.*, 2017; Gao *et al.*, 2018). However, there were considerable differences in the SIC-SOC relationship between regions. For example, the slope in the linear relationship showed a range of 1.84-3.06 in the croplands of north China (Wang *et al.*, 2015b; Guo *et al.*, 2016; Shi *et al.*, 2017), with the greatest slope in saline-alkali soils of the arid region. A complete understanding of this SIC variability is still lacking.

Soil inorganic carbon consists of lithogenic carbonate (LIC) and pedogenic carbonate (PIC). The former is primarily the weathering products of limestone/parent materials. However, PIC is formed mainly through two pathways, i.e. (1) dissolution and re-precipitation of LIC, and (2) dissolution of CO_2 then precipitation with

Ca^{2+}/Mg^{2+} derived from silicate minerals, dust and chemical fertilizers (Monger *et al.*, 2015; Wang *et al.*, 2018). Therefore, PIC formation may be attributable to SIC variability, and it is crucial to understand the dynamics of PIC in various ecosystems.

There have been limited studies quantifying PIC in the vast arid, semi-arid, and semi-humid regions, which show large variations in terms of PIC stock and its contribution to SIC stock (Wang *et al.*, 2014; Bughio *et al.*, 2016; Gao *et al.*, 2017). There is evidence that PIC stock exceeds SOC stock in the upper 1 m, e.g. in the shrub land and cropland in north China (Wang et al., 2015b), and in prairies and forest soils in Canada (Landi et al., 2003). Limited studies showed that the contribution of PIC to SIC was significantly higher in croplands than in shrub lands (Wang *et al.*, 2015b) and grasslands in the northwest China (Yang et al., 2018). The limited reports imply that intensive cropping may lead to PIC formation in the north China, and sound agricultural practice can enhance carbon storage in soil profile, not only as SOC but also as carbonate.

Based on a few long-term experiments, the contribution of PIC to SIC varies greatly (from 29% to 89%) in the cropland of north China (Wang *et al.*, 2014; Wang *et al.*, 2015b; Bughio *et al.*, 2016), which may reflect the differences in cropping, fertilization, climatic condition and soil properties. In this study, we select the North China Plain, the main food producing region in China, which is under similar climate with the same parent material. There has been intensive cropping in majority of the land except in the Yellow River Delta (YRD) that is under varying degrees of salinization. The objectives of this study are to evaluate the spatial distribution of PIC in the typical cropland of the North China Plain, and to test the hypothesis that PIC is influenced by intensive cropping and salinization.

2. Materials and methods

2.1 Description of the study area

The study area includes the Hebei Plain (HBP) and the YRD, which is influenced by the Eurasian east coast temperate monsoon system, with a cold and dry winter, hot and rainy summer, and a severely dry spring. The elevation is less than 50 m in the HBP and 6-15 m in the YRD. Annual mean temperature is 12.5°C and 13.4°C, annual mean precipitation 550 mm and 600 mm, and annual mean evaporation 1900 and 2500 mm in the HBP and YRD, respectively. There is an overall west-to-east elevation in groundwater table and soil salinity (Wang *et al.*, 2012), indicating that the YRD is influenced by hydrological process and has higher salinity relative to the HBP.

Majority of the soils in the study were developed on alluvial loess. Main soil types in the HBP are Ochri-Aquic Camosols and Endorusti-Ustic Cambosols based on the Chinese soil classification system (1995), or Calcaric Cambisol and Fluvo-Aquic according to the FAO-UNESCO system (1988). Soils in the YRD are mainly classified as Salic Fluvisols, Calcaric Fluvisols and Gleyic Solonchaks (Fang *et al.*, 2005). Soil texture is similar across the study area, containing ~17% clay (< 0.002 mm), ~66% silt (0.002-0.02 mm), and ~17% sand (0.02-2 mm). The majority cropland has a double cropping system growing winter wheat and summer maize, which is irrigated with underground water and/or river water from the Yellow River. Conventional tillage has been applied, with a plough depth varying from 20 cm to 30 cm. Farmers often apply mineral nitrogen-phosphorus fertilizers (sometime with organic amendments such as manure application and straw incorporation). There are not significant differences in total nitrogen (TN) and C:N ratio in surface soils between the two regions, i.e., an average of 1.12 g/kg and 9.1 in the HBP, and 1.04

g/kg and 8.9 in the YRD (Table 1).

2.2 Soil sampling and analyses

We selected 23 representative sites: 11 sites in the HBP and 12 sites in the YRD. At each site, 3-4 soil profiles (100 cm in depth) were randomly selected, which were spaced by >100 meters. Soil samples were collected using a soil auger (5 cm in diameter) at intervals of 20 cm, and mixed for the same layer from 3-4 soil profiles. Soils were air-dried, mixed thoroughly and passed through a 2-mm screen.

We measured soil pH, total dissolved solid (TDS) and electrical conductivity (EC) in a soil-water mixture (1:5), and water-soluble Ca^{2+} and Mg^{2+} using an Atomic Absorption Spectrometry by ICP-MS. Subsamples were ground to 0.25-mm and used to analyze total soil carbon, SOC and TN using a CNHS–O analyzer (Model EuroEA3000). In brief, SOC was determined by soaking 1g soil in 10 ml 1N HCI for 12 hr to ensure carbonate removed, followed by combustion at 1020°C under a constant flow of helium carrying pure oxygen, and determination of CO_2 production using a thermal conductivity detector. We used a similar method to determine total soil carbon, but without removing carbonate. We calculated SIC by subtracting SOC from total soil carbon. To determining stable ^{13}C isotopic compositions in SOC ($\delta^{13}C_{org}$), a pretreatment was carried out by treating a freeze-dried sample (about 0.2g) with 10 ml 2N HCI for 24h (to remove carbonate), and followed by washing with deionized water (until pH reached 7) then drying (at 45 ° C). ^{13}C value in the pre-treated sample was measured using a Thermo-elemental analyzer combined with an isotope ratio mass spectrometer (Thermo Finnigan MAT, Delta Plus XP, Germany). The stable isotopic compositions in SIC ($\delta^{13}C_{carb}$) was determined after full reaction with 100% H_3PO_4 using a Thermo-Fisher MAT 253 Isotope Ratio Mass Spectrometer.

The stable isotopic compositions are expressed as:

$$\delta^{13}C = \left(\frac{R_s}{R_{st}} - 1\right) \times 1000 \qquad (1)$$

where R_s is the ^{13}C:^{12}C ratio in the sample, and R_{st} the ratio in the Vienna Pee Dee Belemnite (VPDB) standard.

2.3 Calculation of pedogenic carbonate content

Stable isotope approach has been widely used to partition PIC from LIC because of their distinctive $\delta^{13}C$ values that reflect their origins (Landi *et al.*, 2003; Breecker *et al.*, 2009). In general, PIC has more negative $\delta^{13}C$ values, which result from the isotopic fractionations during the formation of PIC (Cerling *et al.*, 1989).

Based on Landi *et al.* (2003), we calculates PIC content as follows:

$$PIC = \frac{\delta^{13}C_{\mathrm{carb}} - \delta^{13}C_{PM}}{\delta^{13}C_{PIC} - \delta^{13}C_{PM}} SIC \qquad (2)$$

where $\delta^{13}C_{carb}$, $\delta^{13}C_{PM}$ and $\delta^{13}C_{PIC}$ represent carbon isotope in total SIC, parent material and pedogenic carbonate, respectively. Following some earlier studies (Liu *et al.*, 2011; Wang *et al.*, 2014), we set the $\delta^{13}C_{PM}$ as -1‰. According to Mermut *et al.* (2000); Wang *et al.* (2014), $\delta^{13}C_{PIC}$ was calculated from the organic carbon isotope $\delta^{13}C_{org}$:

$$\delta^{13}C_{PIC} = \delta^{13}C_{org} + 14.9 \qquad (3)$$

where the value 14.9 is the total isotope fractionation of 10.5‰ for carbonate precipitation plus 4.4‰ for CO_2 diffusion (Cerling, 1984; Cerling *et al.*, 1989).

2.4 Statistical analyses

We conducted one-way analysis of variance (ANOVA) with least significant difference (LSD) for the comparisons of soil carbon and other properties between layers and regions. Sperman rank correlation analysis and linear regression were applied to explore the relationship between soil carbon stocks. All statistical analyses were conducted using the SPSS19.0.

3. Results

3.1 Comparison of basic soil properties

There was a large spatial distribution in soil pH, TDS and water soluble Ca^{2+} and Mg^{2+}, and the spatial pattern differed greatly among these variables (Figure 1). On average, soil pH was significantly higher in the HBP (8.45-8.64) than in the YRD (8.17-8.35), with relatively lower values found over 0-20 cm (Table 1). However, TDS and water soluble Ca^{2+} and Mg^{2+} were significantly lower in the HBP than in the YRD, with the largest differences seen over 0-20 cm for Ca^{2+} and Mg^{2+}. In particular, TDS and water soluble Ca were ~100% higher in the YRD than in the HBP in the surface soil. While most variables showed a general increasing trend with depth, water soluble Ca revealed an opposite trend (i.e. decreasing from 116 mg kg^{-1} in the 0-20 cm layer to 93 mg kg^{-1} in the 80-100 cm layer).

There was no significant difference in SOC, TN and C:N ratio between the two regions except that the SOC content was significantly higher in the HBP (2.7-9.7 g kg^{-1}) than in the YRD (2.0-8.9 g kg^{-1}) in the 0-20 and 80-100 cm layers (Table 1). Interestingly, the two regions revealed the same degree of decline (from 0-20 cm to 80-100 cm) for both SOC (i.e., ~6.9 g kg^{-1}) and TN (i.e., 0.7 g kg^{-1}). Soil C:N ratio showed a significant decrease with depth, i.e., from 8.9-9.1 in the 0-20 cm layer to 7.4-7.6 in the 80-100cm layer.

3.2 Comparisons of carbonate and carbon isotope

There was considerable spatial variability in the $\delta^{13}C_{org}$ value (Figure 2), which was more negative close to the Yellow River, particularly over 40-100 cm (Figure 2e). There were considerable differences in the spatial distribution between $\delta^{13}C_{carb}$ and $\delta^{13}C_{org}$. The most negative $\delta^{13}C_{carb}$ values were found at the two sites distant from the Yellow River, and less negative values in the lower reaches of the YRD (Figure 2d and 2f). While $\delta^{13}C_{carb}$ ranged from -3.2‰ to -7.1‰, most sites showed a value between -4‰ and -5‰.

On average, $\delta^{13}C$ of SOC was significantly more negative throughout the whole soil profile in the YRD (-22.2‰ to -23.58‰) than in the HBP (-21.5‰ to -22‰) (Table2). On the contrary, $\delta^{13}C$ of SIC was more negative in the HBP (-4.6‰ to -4.9‰) than in the YRD (-4.3‰ to -4.6‰). Overall, ^{13}C was depleted for both SOC and SIC in the deep soils in both regions, with the greatest depletion found in SOC (>1‰) in the YRD.

Unlike SOC, SIC content was significantly higher in the YRD (11.1-12.2 g kg^{-1}) than in the HBP (7.4-10.0 g kg^{-1}), with the largest difference (3.7 g kg^{-1}) found above 20 cm, and the smallest difference (1.7 g kg^{-1}) below 80 cm (Table 2). There was a significant increase with depth in the HBP, with a significant increase found only in the80-100 cm layer. The contribution of PIC to SIC was significantly greater in the HBP (62-66%) than in the YRD (48-55%), with the lowest percentage found over 80-100 cm in the YRD. There were significant differences in PIC between the two regions, with relatively higher values over 0-60 cm but lower values over 80-100 cm in the YRD. LIC content was significantly greater in the YRD (5.3-6.1 g kg^{-1}) than in the HBP (2.8-3.3 g kg^{-1}).

3.3 Spatial distributions of SOC and PIC

There was a lager spatial variability in SOC, with a range of 5.6-19.7, 2.2-10.1 and 1.1-6.6 kg C m^{-3} in the 0-20, 20-40, and 40-100 cm layers, respectively (Figure 3a,c,e). The topsoil (0-20 cm) showed relatively higher SOC levels (>13 kg C m^{-3}) to the west (near the Taihang Mountain) and in the upper YRD (Figure 2a). While the spatial distribution of SOC was somewhat different in the 20-40 cm and 40-100 cm layers, there was considerable similarity in that of YRD, i.e. a decreasing trend from the upper YRD to the lower YRD.

PIC also showed large spatial variability, which varied from 3.4 to 14.8 kg C m^{-3} in the 0-20 cm layer, 3.6 to 13.4 kg C m^{-3} in the 20-40 cm layer, and from 3.8 to 14.3 kg C m^{-3} in layers between 40 and 100 cm (Figure 3bdf). There were some differences in the spatial distribution of PIC among layers, particularly in the HBP; however, there was a degree of similarity near the Yellow River, e.g. extremely low values in the lower YRD. Overall, the spatial distribution was similar in the YRD, but different in the HBP between PIC and SOC.

4. Discussion

4.1 Influences of salinization on soil carbon

Our data show that soils have significantly higher levels of salts in the YRD than in the HBP (Table 1). Generally, plant growth is poor in salt-affected soils due to unfavorable physical and chemical conditions, which leads to low biomass, thus lower inputs of organic materials and low levels of SOC (Demoling *et al.*, 2007; Ding *et al.*, 2016; Chen *et al.*, 2017). Interestingly, our analyses show that SOC is significantly lower in the YRD compared to the HBP only in the 0-20 and 80-100 cm layers. Nevertheless, we conducted the correlation analysis between TDS and SOC, which showed a significant ($P<0.05$) negative correlation (Figure S1). There are a few mechanisms that may lead to lower SOC (e.g., higher decomposition rate). There is evidence that decomposition rate of SOC is low in salt-affected soils because microbial activities are inhibited by the salty environments (Aon and Colaneri, 2001; Wong *et al.*, 2010; Mavi *et al.*, 2012; Thiele-Bruhn *et al.*, 2012; Yan and Marschner, 2013). Generally, decomposition leads to enriched ^{13}C in SOC due to isotopic fractionation (Ågren *et al.*, 1996; Wynn *et al.*, 2005). Indeed, we find that there is significant ^{13}C enrichment (by 0.5-1.6‰) in SOC in the HBP relative to the YRD, implying that other processes rather than decomposition are responsible for the lower SOC in the YRD. In general, cultivation history is shorter in the YRD than in the HBP (Fang *et al.*, 2005; Ju *et al.*, 2009), which would lead to relatively lower SOC in the YRD. In addition, stronger hydrological processes with high salinity in the YRD would cause desorption and transportation of dissolved organic carbon (Mavi *et al.*, 2012), also leading to lower levels of SOC in soil profiles particularly in the subsoils (Shi *et al.*, 2017).

Unlike SOC, SIC content is significantly greater in the salt-affected soils of the YRD relative to the HBP, with the largest difference in the topsoil. Overall, the vertical variation and magnitude of SIC in the YRD of our study are similar to those in the upper YRD reported by Guo *et al.* (2016). Previous studies have suggested that high levels of Ca^{2+} and Mg^{2+} in high pH soils may result in enhanced carbonate precipitation (Wang *et al.*, 2015a; Guo *et al.*, 2016; Rowley *et al.*, 2018). Our data show that water-soluble Ca^{2+} and Mg^{2+} contents are much higher in the YRD than in the HBP, particularly in the topsoil. It appears that higher SIC levels correspond to high levels of Ca^{2+} and Mg^{2+} in our study area. However, there is no significant correlation between SIC and Ca^{2+}/Mg^{2+}, which is inconsistent with the findings of Guo *et al.* (2016).Other factors/variables could have complex influences on the precipitation and dissolution of SIC (Monger *et al.*, 2015).

Generally, more negative $\delta^{13}C$ in SIC indicates higher levels of PIC thus more carbonate Neo-formation (Stevenson *et al.*, 2005; Wang *et al.*, 2014). Accordingly, it is reasonable to assume that there should be more PIC formed during the long history of cropping in the HBP which shows a more negative $\delta^{13}C$ value in SIC. While the contribution of PIC to SIC is significantly larger in the HBP (64-71%) than in the YRD (48-55%), PIC content is slightly lower in the former than in the latter above 60 cm, which is probably related to the difference in Ca^{2+} and Mg^{2+} contents. On the other hand, the observed lower SIC in the HBP (particularly in the upper layer) may also partly result from dissolution of carbonate in association with fertilization and irrigation, and more CO_2 production due to decomposition of SOM and root respiration during long history of cropping (Li *et al.*, 2010; Zamanian *et al.*, 2016; Zhao *et al.*, 2016). Given that SIC content is significantly greater below 80 cm than in the upper layer in the HBP, it is likely to have even higher levels of SIC below 100 cm in this loess soil. An earlier study has demonstrated that there is a large amount of SIC even below 2 m in the Loess Plateau (Zhang *et al.*, 2015). Therefore, future studies on soil carbonate dynamics should include assessments of deep soil.

4.2 Relationship between soil carbonate and SOC

A number of studies evaluating the SIC-SOC relationship in the north China have shown a negative correlation for topsoil in croplands and grasslands (Zhang *et al.*, 2015; Zhao *et al.*, 2016), but a positive correlation in croplands for the upper 1 m (Wang *et al.*, 2015b; Guo *et al.*, 2016; Shi *et al.*, 2017). However, Figure 4 illustrates that there is no significant SIC-SOC correlation in either the 0-20 cm or 0-100 cm in the croplands of HBP and YRD, which is inconsistent with the findings reported for the upper YRD (Guo *et al.*, 2016) and HBP (Shi *et al.*, 2017). This study uses about half of the samples from Shi *et al.* (2017)'s study in the HBP, and the sampling area covers the entire YRD with much lower density compared to the study of Guo *et al.* (2016). Interestingly, SOC and SIC contents in the YRD from this study are close to those reported by Guo *et al.* (2016); vertical variation and magnitude of SOC content are also similar for the HBP between this study and Shi *et al.* (2017)'s study. Not surprisingly, SIC content in the HBP is a bit lower in our study than in Shi *et al.* (2017)'s study that includes a few sites near the Yellow River.

Our regression analyses show a significant positive relationship between PIC and SOC over 0-20 cm in both HBP and YRD, and over the 0-100 cm profile in the YRD (Figure 4b and 4d). The combined data yields a significant (p < 0.01) positive correlation between PIC and SOC over 0-100 cm, which has a much smaller slope (0.65 vs. 1.89) and larger intercept (4.96 vs. -0.94) relative to that in the Yanqi Basin (Wang *et al.*, 2015b). Note that the PIC-SOC relationship in Wang *et al.* (2015b) was derived using data from various land uses.

There are limited studies that quantify both PIC and SOC stocks in the croplands of north China (Figure 5). While there are considerable variations in the carbon stocks, there is an overall positive relationship (p=0.15) between PIC and SOC stocks in the upper 1 m profile. Interestingly, the slope of 1.99 is close to that (1.89) reported for the Yanqi Basin (Wang *et al.*, 2015b), implying that an increase in SOC stock may result in an even greater increase in PIC in arid, semi-arid and semi-humid regions.

4.3 Mechanisms underlying PIC variability in the cropland of north China

The limited PIC data in the croplands of north China are from long-term experiments (i.e. Urmuqi, Yangling, Zhengzhou and Quzhou) and field survey (Yanqi Basin)

(Table 3). The long-term experiments often receive plenty of irrigation, which may enhance carbonate dissolution and downward movement. Overall, PIC stocks and PIC:SOC ratios are relatively low (<5 kg C m^{-2} and <1) under long-term experiments, except at Yangling which had a very low E:P ratio (2.56) and the highest SOC stock (8.64 kg C m^{-2}). The mean PIC stocks in the HBP (9.41 kg C m^{-2}) and YRD (8.67 kg C m^{-2}) are significantly higher than previously reported values for Quzhou (4.1 kg C m^{-2}) and Zhengzhou (4.53 kg C m^{-2}), but are comparable to the value of 9.44 kg C m^{-2} in Yangling, which has the same cropping system, same/similar parent material and similar climate conditions. However, our estimates are significantly lower than that in the cropland of the Yanqi Basin (18.6 kg C m^{-2}) that has a different parent material (Limestone) and a much higher E:P ratio (>25) than our study region.

Carbonate formation and dissolution are associated with the following reactions:

$$CO_2 + H_2O \leftrightarrow HCO_3{}^- + H^+ \quad (5)$$

$$Ca^{2+} + 2HCO_3{}^- \leftrightarrow CaCO_3 + H_2O + CO_2 \quad (6)$$

While both the YRD and the Yanqi Basin have saline soils with similar pH, SOC content is much higher in the Yanqi Basin. The high SOC level and rich Ca^{2+}/Mg^{2+} provide essential materials for PIC formation in the Yanqi Basin (Wang *et al.*, 2015b), and the dry climate conditions (i.e., E:P >25) are not suitable for carbonate dissolution and leaching, which leads to PIC accumulation (Monger *et al.*, 2015; Zamanian *et al.*, 2016). Although the YRD's soils are also rich in Ca^{2+}/Mg^{2+}, other environmental conditions may have adverse effects on PIC accumulation. In particular, CO_2 production is low in salt-affected soils (Wong *et al.*, 2010), which would have less carbonate dissolution in topsoil thus less precipitation in subsoil. In addition, the salty environment can enhance desorption of dissolved organic carbon, and leaching of various dissolved materials (e.g., $HCO_3{}^-$, Ca^{2+}/Mg^{2+}) in semi-humid regions

(Amundson *et al.*, 1994; Bughio *et al.*, 2016), leading to less formation of PIC in soil profile. As a result, the PIC:SOC ratio is significantly smaller in the YRD (1.53) than in the Yanqi Basin (2.02).

4.4 Conclusion

We studies soil carbon dynamics in the typical wheat-maize cropland of North China Plain that consists of two main regions, i.e., HBP and YRD, with similar climate conditions and parent materials. Overall, salt and Ca^{2+}/Mg^{2+} contents were significantly higher in the YRD than in HBP, particularly in top soils. SOC content was significantly lower in 0-20 cm and 80-100 cm layers in the YRD than in HBP, which might be resulted from shorter cultivation history and higher salinity in the YRD. In contrast, SIC content was much higher in the YRD (11-12 g kg^{-1}) than in the HBP (7.4-10 g kg^{-1}), with the largest difference found in topsoil. While the higher SIC levels in the YRD might be related to the high levels of Ca^{2+} and Mg^{2+} in soil profiles, the lower SIC levels in the HBP could partly result from dissolution of carbonate (mainly LIC) during long history of cropping with fertilization and irrigation. Despite of some decreases of PIC content in the upper 60 cm of HBP, PIC stock over 0-100 cm was significantly higher in HBP relative to YRD. There was a significant positive correlation between PIC and SOC stocks in the North China Plain, and an overall positive relationship between PIC and SOC in north China's cropland, which implies that an increase of SOC may enhance the formation of PIC.

Apparently, the formation and transformation of carbonate in the croplands of north China are regulated by many factors. While high soil pH (often >8) and salty environments (with high levels of Ca^{2+} and Mg^{2+}) are essential conditions beneficial for carbonate precipitation, hydrological processes can influence the biological, chemical and physical processes associated with the transformations of organic and inorganic carbon, which leads to complex impacts on the dissolution and precipitation of carbonate in salt-affected soils. On the other hand, intensive cropping with sound management would not only increase SOC stock but also PIC accumulation in arid, semi-arid and semi-humid lands. Future studies with quantitative approaches are needed to advance our understanding of accumulation and transformation of various carbon forms in croplands.

Acknowledgements

This research was supported by the National Natural Science Foundation of China (41877028). The input of Pete Smith contributes to the UK-China Virtual Joint Centre on Nitrogen, N-Circle (BB/N013484/1), funded under the Newton Fund, and the NERC-funded project Soils-R-GRREAT (NE/P019455/1). The authors have no conflict of interest to declare.

References

Ågren, G.I., Bosatta, E., Balesdent, J., 1996. Isotope Discrimination during Decomposition of Organic Matter: A Theoretical Analysis. Soil Science Society of America Journal 60, 1121-1126.

Amundson, R., Wang, Y., Chadwick, O., Trumbore, S., Mcfadden, L., Mcdonald, E., Wells, S., Deniro, M., 1994. Factors and processes governing the C-14 content of carbonate in desert soils. Earth & Planetary Science Letters 125, 385-405.

Andriamananjara, A., Hewson, J., Razakamanarivo, H., Andrisoa, R.H., Ranaivoson, N., Ramboatiana, N., Razafindrakoto, M., Ramifehiarivo, N., Razafimanantsoa, M.P., Rabeharisoa, L., 2016. Land cover impacts on aboveground and soil carbon stocks in Malagasy rainforest. Agriculture Ecosystems & Environment 233, 1-15.

Aon, M.A., Colaneri, A.C., 2001. II. Temporal and spatial evolution of enzymatic activities and physico-chemical properties in an agricultural soil. Applied Soil Ecology 18, 255-270.

Breecker, D., Sharp, Z.D., Mcfadden, L., 2009. Seasonal bias in the formation and stable isotope composition of pedogenic carbonate in modern soils from central New Mexico. Geological Society of America Bulletin 121, 630-640.

Bughio, M.A., Wang, P., Meng, F., Qing, C., Kuzyakov, Y., Wang, X., Junejo, S.A., 2016. Neoformation of pedogenic carbonates by irrigation and fertilization and their contribution to carbon sequestration in soil. Geoderma 262, 12-19.

Cerling, T.E., 1984. The stable isotopic composition of modern soil carbonate and its relationship to climate. Earth and Planetary Science Letters 71, 229-240.

Cerling, T.E., Quade, J., Wang, Y., Bowman, J.R., 1989. Carbon isotopes in soils and palaeosols as ecology and palaeoecology indicators. Nature 341, 138-139.

Chen, D., Yuan, L., Liu, Y., Ji, J., Hou, H., 2017. Long-term application of manures plus chemical fertilizers sustained high rice yield and improved soil chemical and bacterial properties. European Journal of Agronomy 90, 34-42.

Demoling, F., Figueroa, D., Bååth, E., 2007. Comparison of factors limiting bacterial growth in different soils. Soil Biology & Biochemistry 39, 2485-2495.

Ding, J., Jiang, X., Ma, M., Zhou, B., Guan, D., Zhao, B., Zhou, J., Cao, F., Li, L., Li, J., 2016. Effect of 35 years inorganic fertilizer and manure amendment on structure of bacterial and archaeal communities in black soil of northeast China. Applied Soil Ecology 105, 187-195.

Don, A., Scholten, T., Schulze, E.D., 2010. Conversion of cropland into grassland: Implications for soil organic - carbon stocks in two soils with different texture. Journal of Plant Nutrition and Soil Science = Zeitschrift fuer Pflanzenernaehrung und Bodenkunde 172, 53-62.

Fang, H., Liu, G., Kearney, M., 2005. Georelational analysis of soil type, soil salt content, landform, and land use in the Yellow River Delta, China. Environmental Management 35, 72-83.

Gao, Y., Dang, P., Zhao, Q., Liu, J., Liu, J., 2018. Effects of vegetation rehabilitation on soil organic and inorganic carbon stocks in the Mu Us Desert, northwest China. Land Degradation & Development 29, 1031-1040.

Gao, Y., Tian, J., Pang, Y., Liu, J., 2017. Soil Inorganic Carbon Sequestration Following Afforestation Is Probably Induced by Pedogenic Carbonate Formation in Northwest China. Front Plant Sci 8, 1282. doi: 1210.3389/fpls.2017.01282.

Guo, Y., Wang, X., Li, X., Wang, J., Xu, M., Li, D., 2016. Dynamics of soil organic and inorganic carbon in the cropland of upper Yellow River Delta, China. Sci Rep 6, 36105. doi: 36110.31038/srep36105.

Ju, X.-T., Xing, G.-X., Chen, X.-P., Zhang, S.-L., Zhang, L.-J., Liu, X.-J., Cui, Z.-L., Yin, B., Christie, P., Zhu, Z.-L., 2009. Reducing environmental risk by improving N management in intensive Chinese agricultural systems. Proceedings of the National Academy of Sciences 106, 3041-3046.

Landi, A., Mermut, A.R., Anderson, D.W., 2003. Origin and rate of pedogenic carbonate accumulation in Saskatchewan soils, Canada. Geoderma 117, 143-156.

Li, G.T., Zhang, C.L., Zhang, H.J., Gilkes, R.J., Prakongkep, N., 2010. Soil inorganic carbon pool changed in long-term fertilization experiments in north China plain. World Congress of Soil Science: Soil Solutions for A Changing World, Brisbane, Australia, 1-6 August 2010. Congress Symposium 4: Greenhouse Gases From Soils, pp. 220-223.

Liu, W., Yang, H., Sun, Y., Wang, X., 2011. δ13C Values of loess total carbonate: A sensitive proxy for Asian summer monsoon in arid northwestern margin of the Chinese loess plateau. Chemical Geology 284, 317-322.

Mavi, M.S., Marschner, P., Chittleborough, D.J., Cox, J.W., Sanderman, J., 2012. Salinity and sodicity affect soil respiration and dissolved organic matter dynamics differentially in soils varying in texture. Soil Biology and Biochemistry 45, 8-13.

Mermut, A.R., Amundson, R., Cerling, T.E., 2000. The use of stable isotopes in studying carbonate dynamics in soils. Global climate change and pedogenic carbonates, 65-85.

Mikhailova, E.A., Post, C.J., 2006. Effects of land use on soil inorganic carbon stocks in the Russian Chernozem. Journal of Environmental Quality 35, 1384. doi: 1310.2134/jeq2005.0151.

Monger, H.C., Kraimer, R.A., Khresat, S.e., Cole, D.R., Wang, X., Wang, J., 2015. Sequestration of inorganic carbon in soil and groundwater. Geology 43, 375-378.

Phillips, R.L., Eken, M.R., West, M.S., 2015. Soil Organic Carbon Beneath Croplands and Re-established Grasslands in the North Dakota Prairie Pothole Region. Environmental Management 55, 1191-1199.

Rowley, M.C., Grand, S., Verrecchia, É.P., 2018. Calcium-mediated stabilisation of soil organic carbon. Biogeochemistry 137, 27-49.

Saha, D., Kukal, S.S., Sharma, S., 2011. Landuse impacts on SOC fractions and aggregate stability in typic ustochrepts of Northwest India. Plant & Soil 339, 457-470.

Shi, H.J., Wang, X.J., Zhao, Y.J., Xu, M.G., Li, D.W., Guo, Y., 2017. Relationship between soil inorganic carbon and organic carbon in the wheat-maize cropland of the North China Plain. Plant and Soil 418, 423-436.

Stevenson, B.A., Kelly, E.F., Mcdonald, E.V., Busacca, A.J., 2005. The stable carbon isotope composition of soil organic carbon and pedogenic carbonates along a bioclimatic gradient in the Palouse region, Washington State, USA. Geoderma 124, 37-47.

Su, Y.Z., Wang, X.F., Yang, R., Lee, J., 2010. Effects of sandy desertified land rehabilitation on soil carbon sequestration and aggregation in an arid region in China. J Environ Manage 91, 2109-2116.

Thiele-Bruhn, S., Bloem, J., Vries, F.T.d., Kalbitz, K., Wagg, C., 2012. Linking soil biodiversity and agricultural soil management ☆. Current Opinion in Environmental Sustainability 4, 523-528.

Wang, J., Zhang, G., Yan, M., Yi, L.I., Zhou, Z., 2012. Analysis of soil salinity distribution and influencing factors in area around Bohai sea. Journal of Arid Land Resources & Environment 11, 107-109.

Wang, J.P., Wang, X.J., Zhang, J., Zhao, C.Y., 2015a. Soil organic and inorganic carbon and stable carbon isotopes in the Yanqi Basin of northwestern China. European Journal of Soil Science 66, 95-103.

Wang, X.J., Wang, J.P., Shi, H.J., Guo, Y., 2018. Carbon Sequestration in Arid Lands: A Mini Review. Springer, Singapore. 133-141, Springer Earth System Sciences.

Wang, X.J., Wang, J.P., Xu, M.G., Zhang, W.J., Fan, T., Zhang, J., 2015b. Carbon accumulation in arid croplands of northwest China: pedogenic carbonate exceeding organic carbon. Sci Rep 5, 11439.

Wang, X.J., Xu, M.G., Wang, J.P., Zhang, W.J., Yang, X.Y., Huang, S.M., Liu, H., 2014. Fertilization enhancing carbon sequestration as carbonate in arid cropland: assessments of long-term experiments in northern China. Plant and Soil 380, 89-100.

Wong, V.N.L., Greene, R.S.B., Dalal, R.C., Murphy, B.W., 2010. Soil carbon dynamics in saline and sodic soils: a review. Soil Use and Management 26, 2-11.

Wu, H., Guo, Z., Gao, Q., Peng, C., 2009. Distribution of soil inorganic carbon storage and its changes due to agricultural land use activity in China. Agriculture, Ecosystems & Environment 129, 413-421.

Wu, H., Guo, Z., Peng, C., 2003. Land use induced changes of organic carbon storage in soils of China. Global Change Biology 9, 305-315.

Wynn, J.G., Bird, M.I., Wong, V.N.L., 2005. Rayleigh distillation and the depth profile of 13 C/ 12 C ratios of soil organic carbon from soils of disparate texture in Iron Range National Park, Far North Queensland, Australia. Geochimica Et Cosmochimica Acta 69, 1961-1973.

Yan, N., Marschner, P., 2013. Response of soil respiration and microbial biomass to changing EC in saline soils. Soil Biology & Biochemistry 65, 322-328.

Yang, F., Huang, L., Yang, R., Yang, F., Li, D., Zhao, Y., Yang, J., Liu, F., Zhang, G., 2018. Vertical distribution and storage of soil organic and inorganic carbon in a typical inland river basin, Northwest China. Journal of Arid Land 10, 183-201.

Zamanian, K., Pustovoytov, K., Kuzyakov, Y., 2016. Pedogenic carbonates: Forms and formation processes. Earth-Science Reviews 157, 1-17.

Zhang, F., Wang, X., Guo, T., Zhang, P., Wang, J., 2015. Soil organic and inorganic carbon in the loess profiles of Lanzhou area: implications of deep soils. Catena 126, 68-74.

Zhang, N., He, X.D., Gao, Y.B., Li, Y.H., Wang, H.T., Di, M.A., Zhang, R., Yang, S., 2010. Pedogenic Carbonate and Soil Dehydrogenase Activity in Response to Soil Organic Matter in Artemisia ordosica Community. Pedosphere 20, 229-235.

Zhao, W., Zhang, R., Huang, C., Wang, B., Cao, H., Koopal, L.K., Tan, W., 2016. Effect of different vegetation cover on the vertical distribution of soil organic and inorganic carbon in the Zhifanggou Watershed on the loess plateau. Catena 139, 191-198.

Table 1. Mean values of soil basic properties in the Hebei Plain (HBP, n=11) and the Yellow River Delta (YRD, n =12)

Layer	pH		TDS (g/kg)		Ca^{2+} (mg/kg)		Mg^{2+} (mg/kg)		SOC (g/kg)		TN (g/kg)		C:N ratio	
(cm)	HBP	YRD	HBP	YRD	HBP	YRD	HBP	YRD	HBP	YRD	HBP	YRD	HBP	YRD
0-20	8.45Aa	8.17Ba	0.3Bc	0.6Ac	55Bc	116Aa	16Bc	27Ab	9.7Aa	8.9Ba	1.1Aa	1.0Aa	9.1Aa	8.9Aa
20-40	8.59Aa	8.33Ba	0.4Bbc	0.7Abc	74Bb	106Aab	24Bb	30Aab	4.0Ab	3.8Ab	0.5Ab	0.5Ab	8.1Aab	7.8Aab
40-60	8.64Aa	8.35Ba	0.5Bb	0.8Ab	74Bb	96Ab	23Bb	30Aab	2.9Ac	3.0Abc	0.4Ab	0.4Ab	7.6Ab	7.5Ab
60-80	8.62Aa	8.31Ba	0.7Bab	1.0Aab	72Bb	95Ab	29Ba	33Aab	2.7Ac	2.5Ac	0.4Ab	0.3Ab	7.6A**b**	7.4Ab
80-100	8.60Aa	8.28Ba	0.8Ba	1.1Aa	90Aa	93Ab	33Aa	35Aa	2.9Ac	2.0Bc	0.4Ab	0.3Ab	7.6Ab	7.4Ab

The same letter (upper case between regions or lower case between soil layers) indicate no significant difference at $P < 0.05$.

Table 2. Mean values of soil carbonate, and stable isotope $\delta^{13}C$ in SOC and SIC in the Hebei Plain (HBP, n=11) and the Yellow River Delta (YRD, n=12)

Layer	δ^{13}Corg		δ^{13}Ccarb		SIC (g/kg)		PIC (%)		PIC (g/kg)		LIC (g/kg)	
(cm)	HBP	YRD	HBP	YRD	HBP	YRD	HBP	YRD	HBP	YRD	HBP	YRD
0-20	-21.52Aa	-22.46Ba	-4.73Ba	-4.33Aa	7.4Bc	11.1Aa	68Aab	52Bab	4.7Bb	5.7Aab	2.8Ba	5.4Aab
20-40	-21.68Ab	-22.20Ba	-4.72Ba	-4.35Aa	8.6Bb	11.4Aa	64Ab	54Bab	5.3Bab	6.1Aab	3.3Ba	5.3Ab
40-60	-21.61Aab	-22.43Ba	-4.64Aa	-4.45Aa	8.7Bb	11.9Aa	67Aab	55Ba	5.6Bab	6.5Aa	3.2Ba	5.4Aab
60-80	-21.51Aa	-23.14Bb	-4.92Bb	-4.45Aa	9.0Bb	12.2Aa	71Aa	50Bab	5.9Aab	6.1Aab	3.0Ba	6.1Aa
80-100	-21.98Ac	-23.58Bb	-4.92Bb	-4.59Ab	10.0Ba	11.7Aa	67Aab	48Bb	6.3Aa	5.6Bb	3.0Ba	6.1Aa

The same letter (upper case between regions or lower case between soil layers) indicate no significant difference at $P < 0.05$.

542

Table 3. Climate and soil properties, and carbon stocks (0-100 cm) in the cropland of north China

Properties	Yanqi Basin[a]	Urmuqi[b]	Yangling[b]	Zhengzhou[b]	Quzhou[c]	Hebei Plain	Yellow River Delta
MAT (°C)	8.5	7.7	13	14.5	13.2	12.5	13.4
MAP (mm)	80	299	585	641	543	550	600
MAE (mm)	>2000	2570	1500	1450	1840	1900	2500
E:P ratio	>25	8.60	2.56	2.26	3.39	3.45	4.17
Parent material	Limestone	Limestone	Loess	River Alluvium	Loess	Loess	River Alluvium
Soil classification (FAO)	Haplic Calcisol	Haplic Calcisol	Calcaric Regosol	Calcaric Cambisol	Fluvic Cambisol	Calcaric Cambisol	Calcaric Fluvisols, Coastalsolonchak
Soil pH	8.29	8.1	8.6	8.3	8.3	8.6	8.2
SOC (kg C m^{-2})	9.20	7.19	8.64	6.85	7.8	6.21	5.65
SIC (kg C m^{-2})	41.90	7.10	12.79	9.74	12.3	13.65	16.87
PIC (kg C m^{-2})	18.60	3.48	9.44	4.53	3.5-4.1	9.41	8.67
LIC (kg C m^{-2})	23.30	3.62	3.35	5.22	8.2	4.24	8.20
PIC:SOC ratio	2.02	0.48	1.09	0.66	0.53	1.52	1.53

MAT: mean annual temperature; MAP: mean annual precipitation; MAE: mean annual evaporation.

[a]Wang *et al.* (2014);

[b]Wang *et al.* (2015b);

[c]Bughio *et al.* (2016).

Figure captions

Figure 1 Spatial distributions of (a) pH, (b) TDS stock, (c) Ca^{2+} stock, and (d) Mg^{2+} stock over 0-100 cm. The figure was generated using ArcMap 10.5 (http://www.esri.com/)

Figure 2 Spatial distributions of δ^{13}Corg (left panel) and δ^{13}Ccarb (right panel) over (a, b) 0-20 cm, (c, d) 20-40 cm, and (e, f) 40-100 cm. The figure was generated using ArcMap 10.5 (http://www.esri.com/).

Figure 3 Spatial distributions of soil organic carbon (SOC) (left panel) and pedogenic carbonate (PIC) stocks (right panel) over (a, b) 0-20 cm, (c, d) 20-40 cm, and (e, f) 40-100 cm. The figure was generated using ArcMap 10.5 (http://www.esri.com/).

Figure 4 Correlation between PIC/SIC and SOC stocks in the Hebei Plain, Yellow River Delta and combined data (blue lines) over (a, b) 0-20 cm, (c, d) 0-100 cm.

Figure 5 Distributions of mean stocks of soil organic carbon (SOC), peodgenic carbonate (PIC) and lithogenic carbonates (LIC) in the 0-100 cm layer in the north China. Data sources were given in Table 3. The figure was generated using ArcMap 10.5 (http://www.esri.com/).

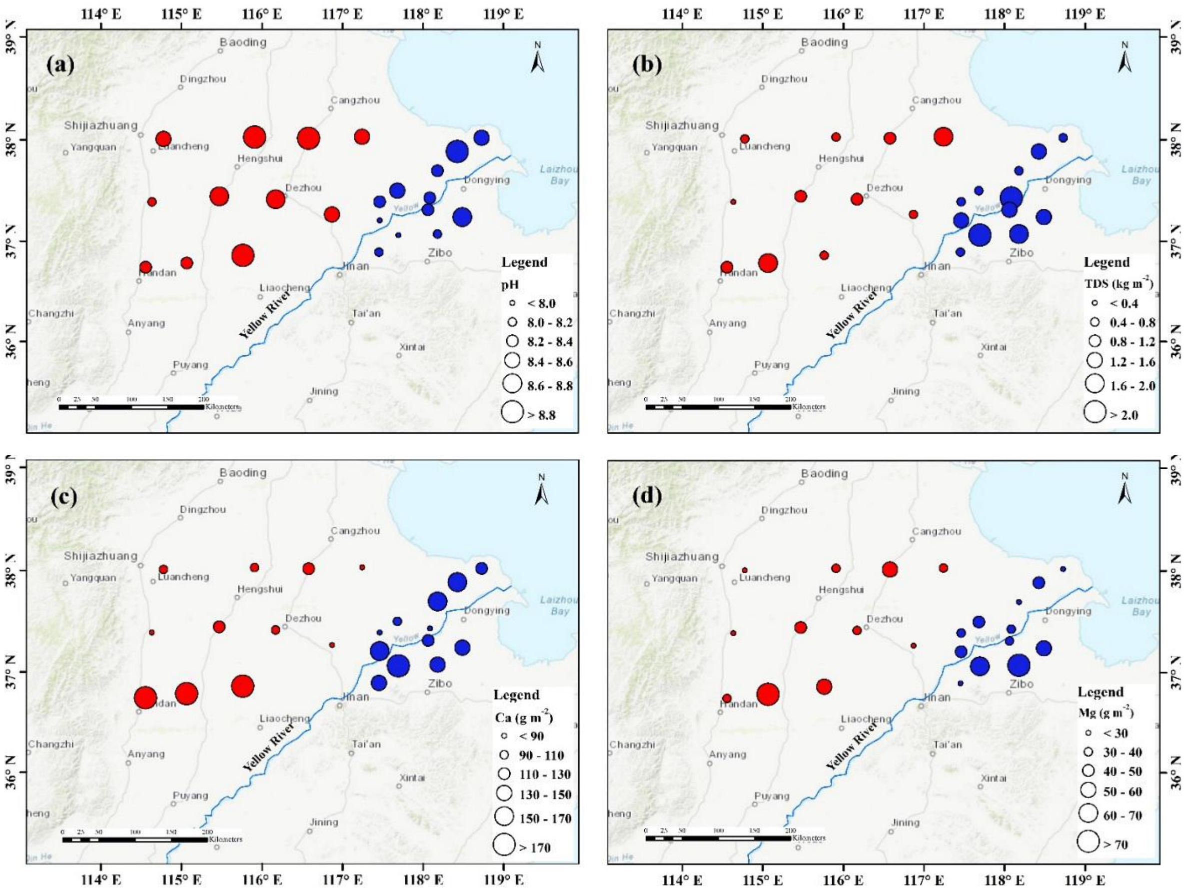

Fig. 1 Spatial distributions of (a) pH, (b) TDS stock, (c) Ca^{2+} stock, and (d) Mg^{2+} stock over 0-100 cm. The figure was generated using ArcMap 10.5 (http://www.esri.com/)

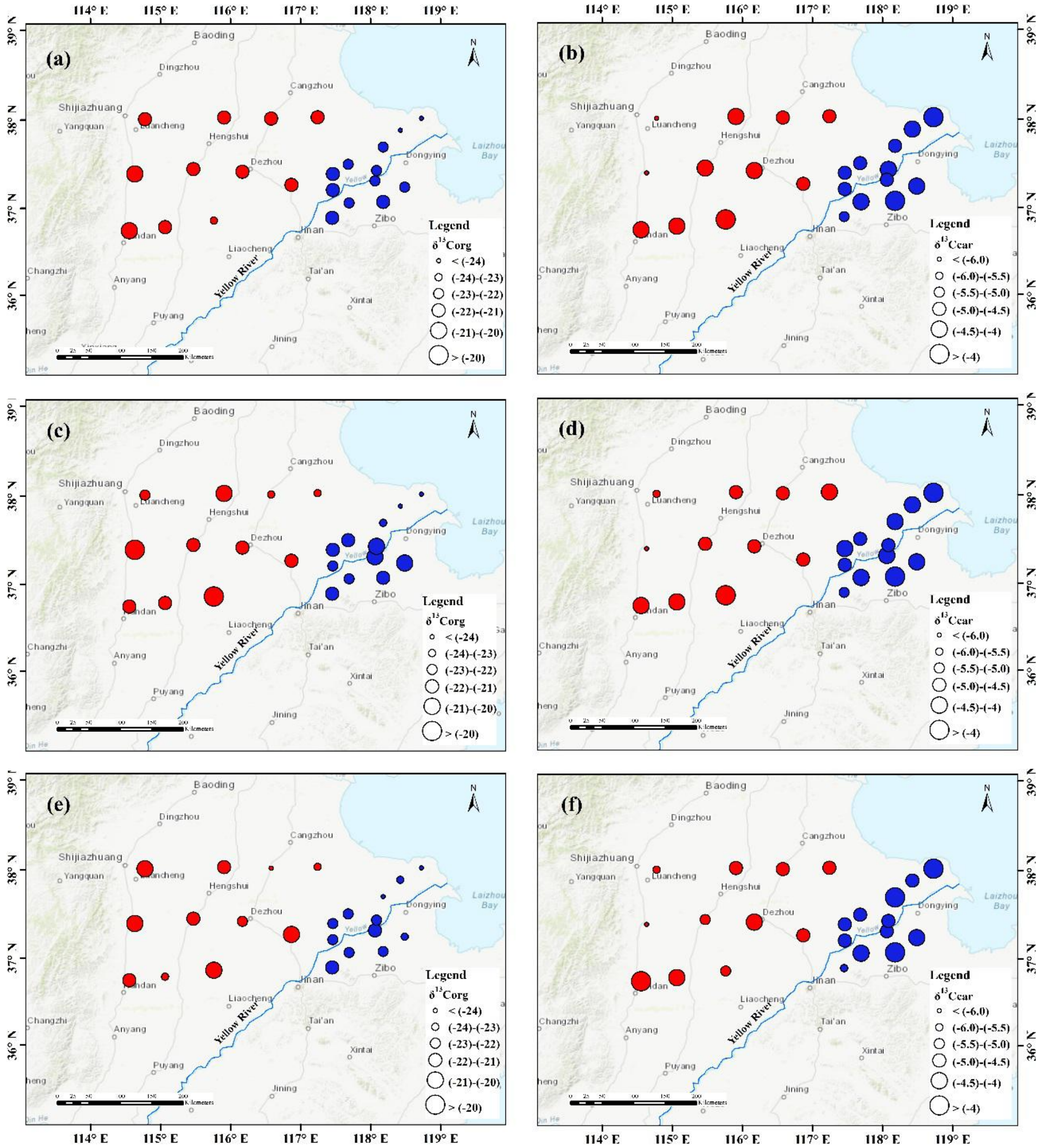

Fig. 2 Spatial distributions of δ^{13}Corg (left panel) and δ^{13}Ccarb (right panel) over (a, b) 0-20 cm, (c, d) 20-40 cm, and (e, f) 40-100 cm. The figure was generated using ArcMap 10.5 (http://www.esri.com/).

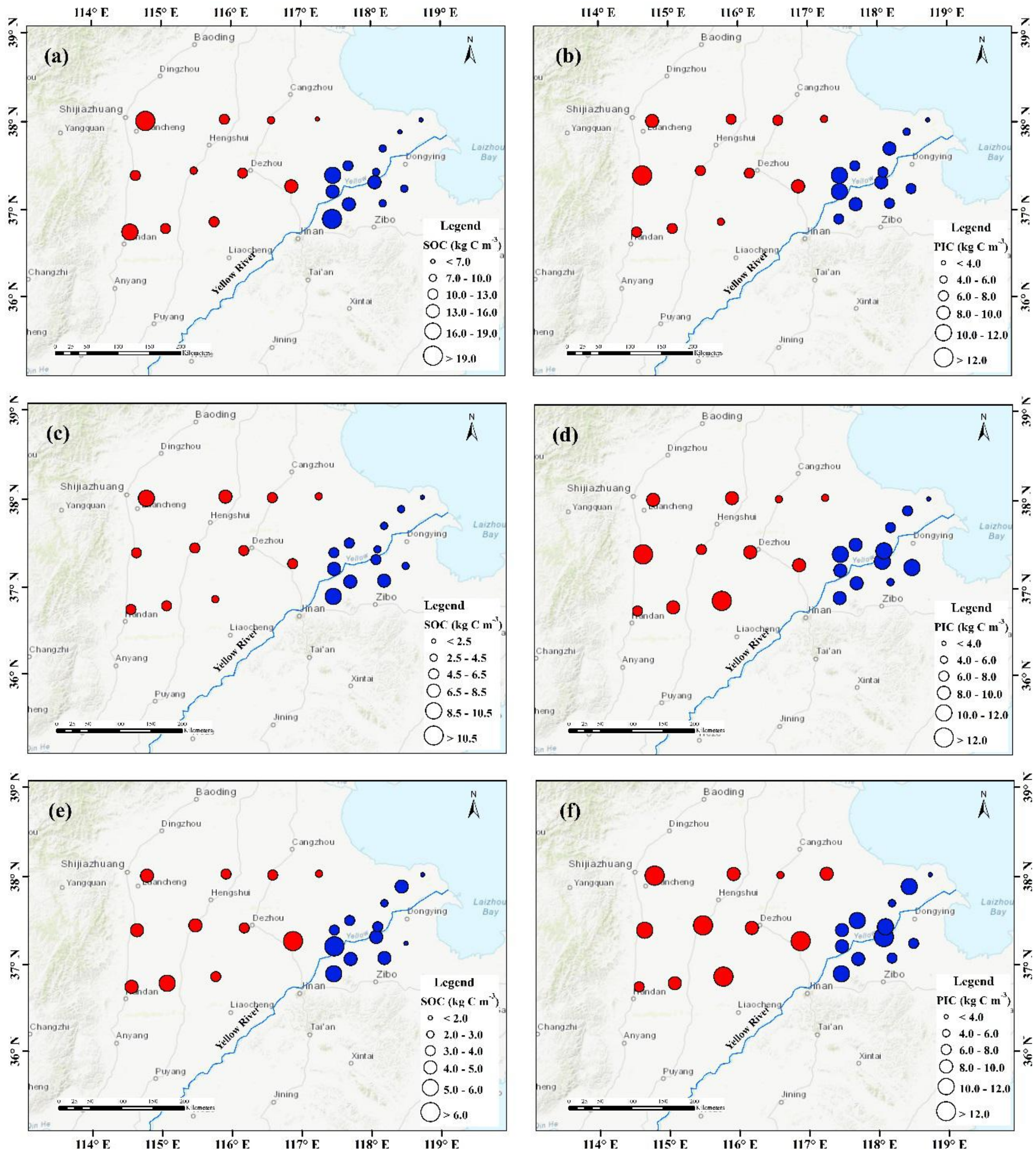

Fig. 3 Spatial distributions of soil organic carbon (SOC) (left panel) and pedogenic carbonate (PIC) stocks (right panel) over (a, b) 0-20 cm, (c, d) 20-40 cm, and (e, f) 40-100 cm. The figure was generated using ArcMap 10.5 (http://www.esri.com/).

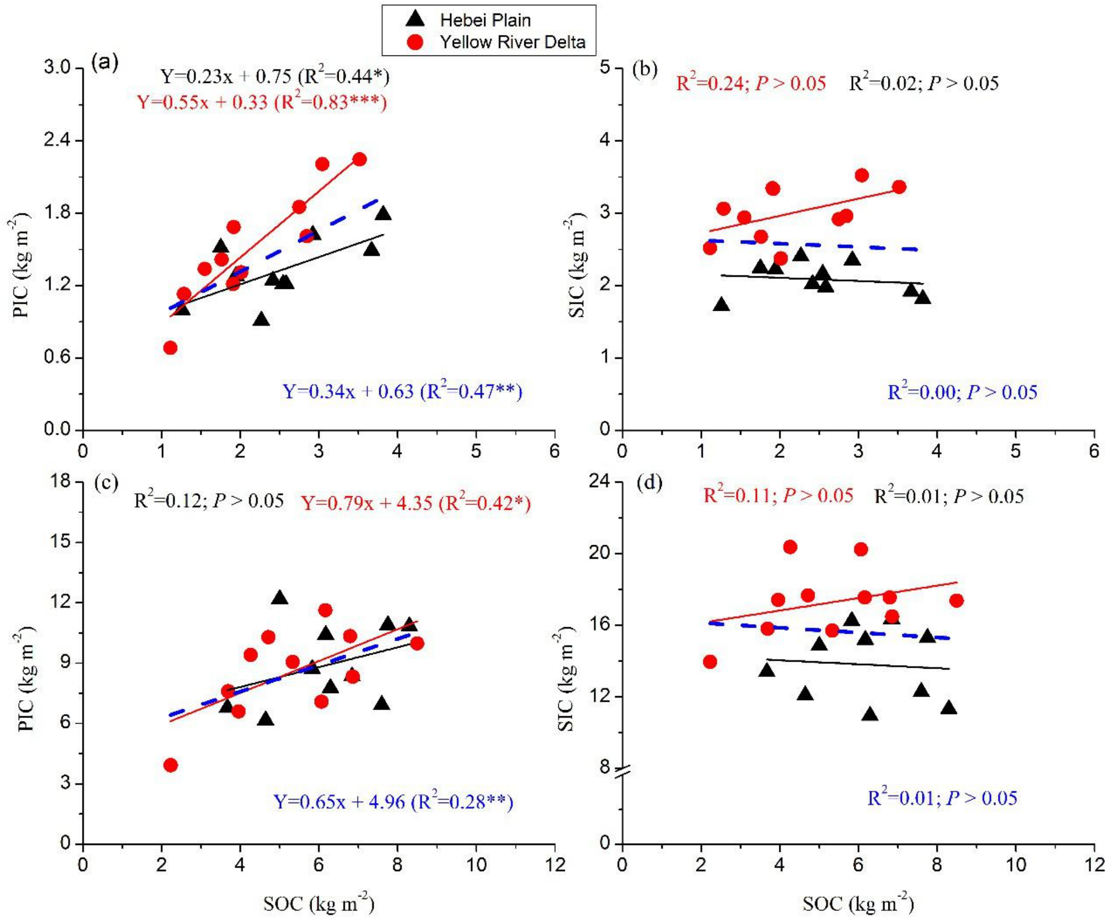

Fig. 4 Correlation between PIC/SIC and SOC stocks in the Hebei Plain, Yellow River Delta and combined data (blue lines) over (a, b) 0-20 cm, (c, d) 0-100 cm.

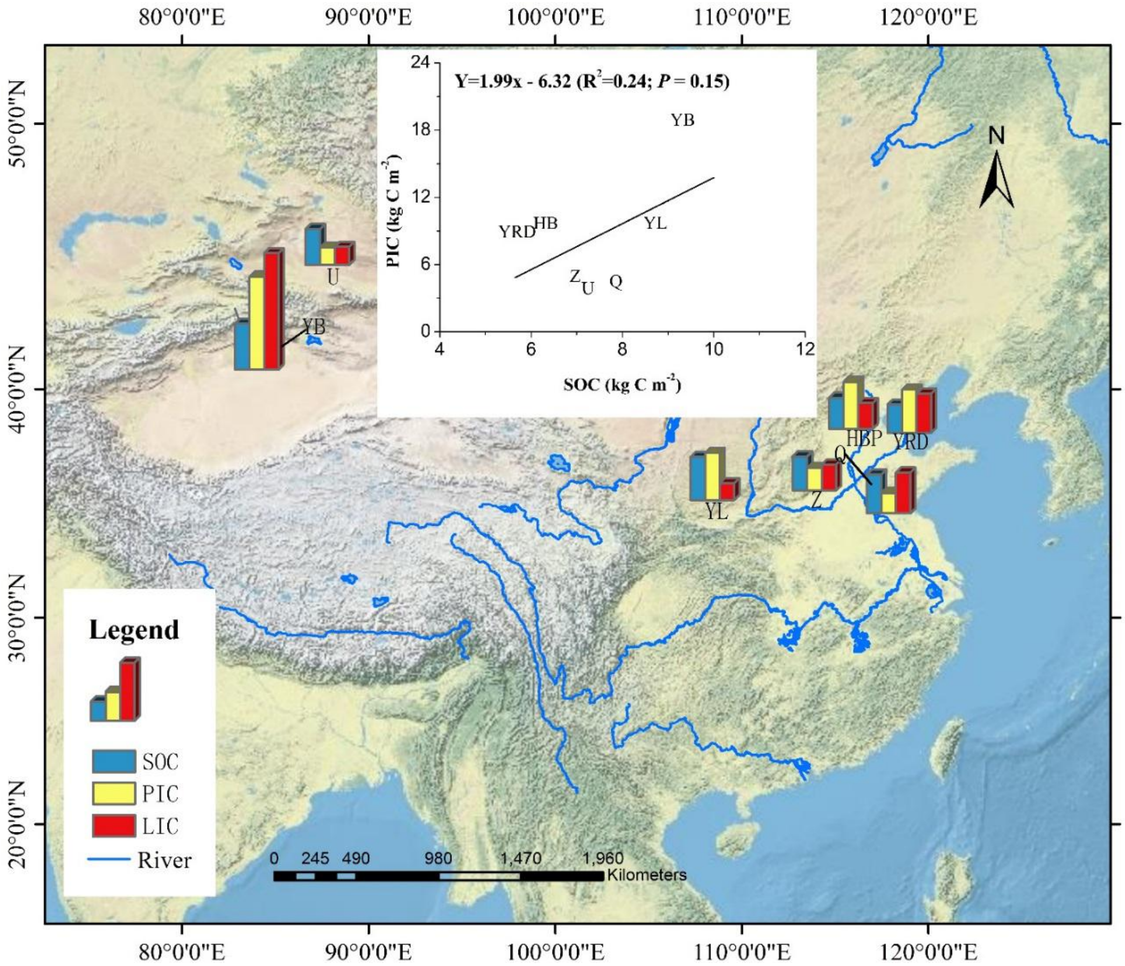

574

575 **Fig. 5** Distributions of mean stocks of soil organic carbon (SOC), peodgenic carbonate (PIC) and
576 lithogenic carbonates (LIC) in the 0-100 cm layer in the north China. Data sources were given in Table
577 3. The figure was generated using ArcMap 10.5 (http://www.esri.com/).